Use of nano-additions to improve the performance of UHPFRCs used in geothermal power plant infrastructures

E. Cuenca[1], A. Mezzena[2] and L. Ferrara[3]

ABSTRACT: The interest of scientific community on application of nano-additions in concrete is continuously growing due to their outstanding physical and chemical properties. These nano-additions are usually added into concrete to increase the durability in aggressive environments, such as XA environmental exposure classes. This work shows preliminary results on the use of nano-additions in an Ultra High Performance Fiber-Reinforced Concrete (UHPFRC) used as a reference. This reference UHPFRC has been modified adding three types of nano-additions: alumina nanofibers (0.25% by weight of cement), cellulose nanocrystals (0.15% by weight of cement) and cellulose nanofibrils (0.15% by weight of cement). The influence of the nano-additions has been analyzed in terms of mechanical properties, such as flexural and compressive strength and on shrinkage and durability properties, analyzed by means of sorptivity tests on uncracked, cracked and self-healed specimens.

1 INTRODUCTION

Reinforced concrete structures exposed to extremely aggressive environments require continuous maintenance all along their service life due to several aging and durability time-dependent problems. The durability of the maintenance interventions has also to be carefully evaluated, since, as shown by Matthews (2007), 50% of the repaired concrete structures failed once again, 25% of which in the first 5 years, 75% within 10 years and 95% within 25 years.

Ultra-high Performance Fiber Reinforced Concrete (UHPFRC) is a well-known class of cementitious composites whose composition is characterized by a high amount of cement and supplementary cementitious materials, such as pozzolan, fly ash and silica fume, fine aggregates and low water/cement ratios (Buttignol et al., 2017). Due to this peculiar composition, such composites have a highly dense and homogeneous micro-structure, with a very low porosity, which, besides resulting into a compressive strength higher than 120-150 MPa, is also conducive to a high durability in the un-cracked state. The presence of steel fibers, added to temper the inherent brittleness, also improves the tensile response in the post-cracking stage, characterized by the development of multiple tiny cracks and tensile strain hardening behavior. The synergy between crack width control due to the fibers and the mix composition as above results very interesting from the point of view of autogenous healing, with healing products repair the cracked area and also improve the matrix-fiber bond (Cuenca and Ferrara, 2017; Cuenca et al., 2018).

The H2020 ReSHEALience project (GA 760824) is working at a "meta-material" Ultra High Durability Concrete approach, where the concept of concrete durability evolves from the role of mere passive provider of protection against the ingress of aggressive agents to that of an active player, able to govern the performance evolution process. A scaling-up is pursued from intrinsic material durability to structural durability, broadly intended as the ability to maintain all along the service life and in the intended scenarios the anticipated level of structural performance, which can be obtained using reduced material quantities thanks to superior mechanical properties (Cuenca et al., 2019; Serna et al., 2019). In this paper preliminary results will be presented on the effects of nano-particles on the performance of a UHPFRC mix to be employed in XA exposure classes.

[1] *Assistant Professor, Politecnico di Milano, estefania.cuenca@polimi.it*
[2] *MSc Building Engineer, Politecnico di Milano alessandro.mezzena@mail.polimi.it*
[3] *Associate Professor, Politecnico di Milano, liberato.ferrara@polimi.it*

2 EXPERIMENTAL PROGRAM

2.1 Concrete mix compositions

A comprehensive experimental campaign focused on the mechanical and durability characterization of Ultra-High Durable Concrete (UHDC) in ordinary and XA exposure conditions has been carried out. The study is based on a reference UHDC with crystalline admixtures (reference mix, XA-CA). In addition, other four mixes have been studied varying some components of the reference mix:

- XA-CA_CEM III: CEM III is used instead of CEM I.
- XA-CA+ANF: 0.25% by cement mass of alumina nanofibers (Al_2O_3) is included to the reference mix (XA-CA).
- XA-CA+CNC: 0.15% by cement mass of cellulose nanocrystals (CNC) is included to the reference mix (XA-CA).
- XA-CA+CNF: 0.15% by cement mass of cellulose nanofibrils (CNF) is included to the reference mix (XA-CA).

Details of the mix compositions are provided in Table 1.

The aluminium oxide nanofibers branded as NAFEN™, employed in this investigation, have been so far applied into a broad range of industrial products (aerospace, automotive, energy), resulting into a confirmed 20-50% improvements in mechanical properties of polymer and composite end products. The fibres are 4 to 11 nm in diameter and from 100 to 900 nm long, with a specific surface equal to 155 m^2/g. In order to be employed into a cementitious composite mix featuring low w/b ratios they need to be supplied into a sonicated suspension at a solid concentration ratio equal to 10%, much higher than for other applications.

As for the cellulose nanoproducts, in this study choice has been made to use BioPlus ® Cellulose Nanofibrils (CNF), with dimensions ranging from 5-20 nm in diameter and 500-2,000+ nm in length, and BioPlus® Cellulose Nanocrystals (CNC), with dimensions ranging from 5 nm in diameter and 50-500 nm in length supplied in sonicated suspension at 10% solid content.

As for the crystalline admixture, Penetron Admix ® has been chosen, whose effects in ordinary concrete as well as in High Performance Fibre Reinforced Cementitious Composites has already been widely checked by the authors' research group (Ferrara et al., 2014; Ferrara et al., 2016) also with reference to exposure to chloride rich environments (Borg et al., 2018; Cuenca et al., 2019).

Table 1. Concrete dosages [kg/m^3]

Constituents	XA-CA	XA-CA _CEMIII	XA-CA +ANF	XA-CA +CNC	XA-CA +CNF
CEM I 52,5 R	*600*	*-*	*600*	*600*	*600*
CEM III	*-*	*600*	*-*	*-*	*-*
Slag	*500*	*500*	*500*	*500*	*500*
Water	*200*	*200*	*200*	*200*	*200*
Steel fibers Azichem Readymesh 200	*120*	*120*	*120*	*120*	*120*
Sand 0-2mm	*982*	*982*	*982*	*982*	*982*
Superplasticizer Glenium ACE 300	*33*	*33*	*33*	*33*	*33*
Crystalline admixtures	*3*	*3*	*3*	*3*	*3*
Alumina nanofibers[*]	*-*	*-*	*0.25*	*-*	*-*
Cellulose nanocrystals[*]	*-*	*-*	*-*	*0.15*	*-*
Cellulose nanofibrils[*]	*-*	*-*	*-*	*-*	*0.15*

[*] *% by cement mass*

2.2 Curing conditions

After casting, specimens were cured in three different curing conditions:

- Standard curing condition in moist room (T=20ºC and RH=95%).
- Immersed in geothermal water, in order to analyze the time evolution of the performance in aggressive acid environments (XA conditions).

The geothermal water comes from the cooling basins of a geothermal power plant owned by Enel Green Power (partner of the ReSHEALience project) in Tuscany. As from performed chemical analysis, this water contains both sulfate and chloride ions (SO_4^{2-} = 2678 ppm and Cl^- = 441 ppm).

2.3 Description of tests

Mechanical and physical characterization tests in ordinary exposure conditions and under and chemical attack XA ones have been performed for all the mixes.
In detail, the tests performed were the following:

- *Flexural and compressive strength tests:* Flexural tests were carried out on prismatic specimens (40x40x160mm). A 5 mm deep notch was cut at mid-span of the specimens, to ease the measurement of the Crack Mouth Opening Displacement (CMOD). Tests were performed in displacement control and the Load vs. CMOD curve was recorded to evaluate also the effects on nano-particles on the toughness of the composites. After flexural tests, the broken halves of prismatic specimens (40x40x160mm) obtained from three-point bending tests, were tested in compression. Flexural and compressive strength tests were performed according to the Standard EN 1015-11:1999. Before the test specimens were cured in moist room and immersion in geothermal water (as explained in Section 2.2). For both curing conditions, tests were performed at 28, 56 and 84 days.
- *Shrinkage tests*: Autogenous and drying (total) shrinkage tests were performed according to 12617-4, keeping the specimens at T = 20°C and RH = 60%
- *Sorptivity tests*: This test, performed according EN 13057:2002 is based on the measurement of the water uptake due to capillary absorption of water over a fixed time interval. The tests were performed in three phases:
  - *Uncracked phase:* After demolding, specimens were kept in moist room. For preconditioning, specimens were oven dried at 40ºC until constant weight was achieved (weight change not greater than 0.2% in 2 hours). Then specimens were kept in the dry room (T=20ºC, RH=60%) for 24 hours. After cooling, specimens were partially waterproofed with silicon to induce a unidirectional flow of water. The waterproofing was applied over a depth of 20mm on both sides and the entire bottom of the specimen except a central 20x40mm area across the notch. Then sorptivity tests were conducted immersing the specimens in tap water. The water level was kept constant at 3mm above the notch tip. The water uptake (mass gain) was measure at regular intervals up to 24 hours. The water uptake (g) was calculated and plotted versus the square root of time. The slope of the water uptake graph is called "sorptivity coefficient (SC)" and is measured in $g/min^{0.5}$.
  - *Cracked phase*: In this phase, specimens were cracked at 28 days with the same 3-point bending setup used for flexural tests. Specimens were cracked up to A CMOD value equal to 150µm. The same procedure for the sorptivity test on uncracked specimens was carried on the cracked specimens.
  - *Healing phase*: The cracked specimens were cured in wet/dry cycles in dry room (T=20ºC and RH=60%) or immersed in geothermal water (as described in Section 2.2). The same procedure for the sorptivity test on uncracked specimens was carried on the specimens after the healing period. In this paper results after one month healing are going to be shown.
- *Self-healing analysis*: The cracked specimens were analyzed by means of optical microscopy visual crack analysis.

3 RESULTS AND DISCUSSION

3.1 Flexural and compressive strength tests

Comparison between average flexural strengths of all mixes cured in the moist room (T =20ºC, RH=95%) is shown in Figure 1(a), whereas Figure 1(b) shows the same comparison with reference to mixes cured in geothermal water. Figure 2(a) shows the comparison between average compressive strengths of all mixes cured in the moist room (T =20ºC, RH=95%), whereas Figure 2(b) shows the comparison between average compressive strengths of all mixes cured in geothermal water.

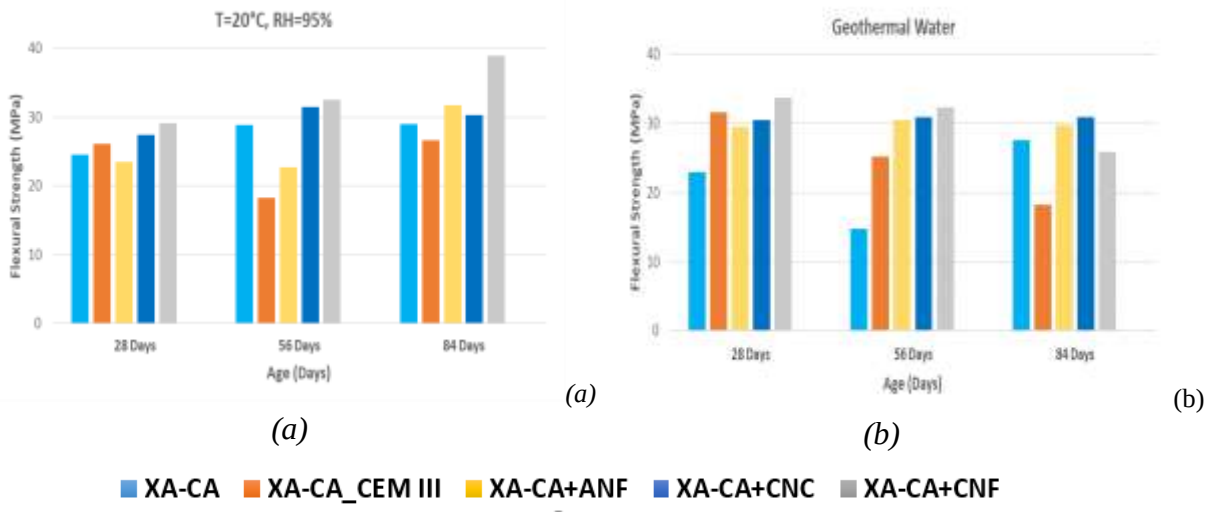

(a) (a) *(b)* (b)

Figure 1. (a) Average flexural strength values of all mixes for specimens cured in moist room (T=20ºC, RH=95%); (b) Average flexural strength values of all mixes for specimens immersed in geothermal water.

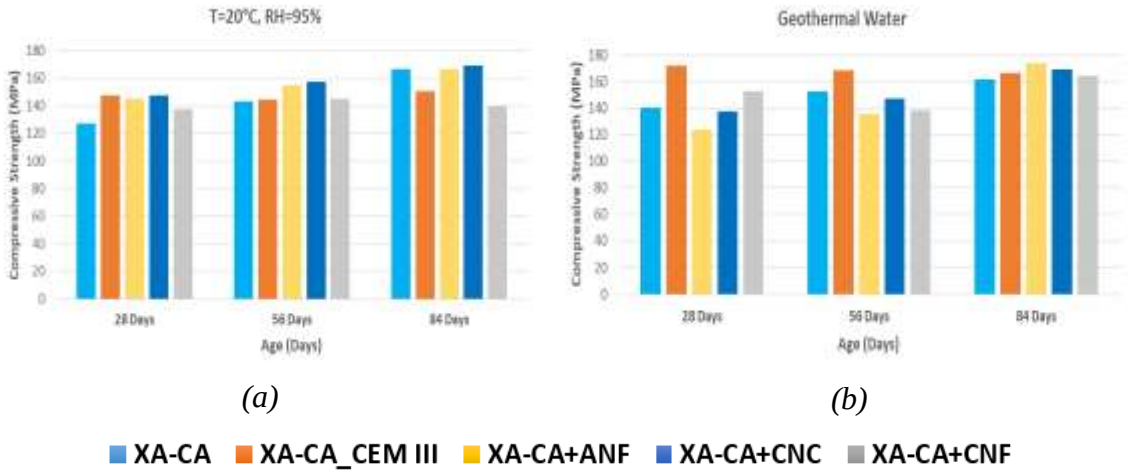

(a) *(b)*

Figure 2. (a) Average compressive strength values of all mixes for specimens cured in moist room (T=20ºC, RH=95%); (b) Average compressive strength values of all mixes for specimens immersed in geothermal water.

Based on the results of both curing environments, it can be concluded that effect of nano-additions to the "compressive strength" is not so significant. Moreover, the effect of exposure conditions is marginal on the compressive strength development. A slight increase of compressive strength in nano-additioned mixes when immersed in geother-

mal water was measured as compared to when cured in climate room (T=20ºC, RH= 95%). On the other hand, according to the results it is evident that the nano-additions perform their best effects on flexural strength when the material is exposed to aggressive environment (immersion in geothermal water), most likely because they are able to interact with the defects (e.g. expansion induced by water with sulfates), at the very onset of their formation.

Moreover, since all the investigated mixes feature a very low porosity with average pore size lower than 10 nm, it can be further hypothesized that both alumina nano-fibres and nano-cellulose crystals/fibrils have the right size to reinforce this "pore-size" and this reinforcement effect may prevent the activation of deterioration reactions triggered by the ingress of aggressive ions (sulfate and chlorides) as above.

3.2 Shrinkage tests

Comparison of autogenous and drying (total) shrinkage are shown in Figure 3(a) and Figure 3(b) respectively for all mixes. Each curve shown in Figure 3(a) and Figure 3(b) represents the average of 3 identical 40x40x160mm specimens. It clearly appears as for such kind of cementitious composites the largest part of the shrinkage deformation is of autogenous type.

XA-CA-CNC (mix with cellulose nanocrystals, CNC) shows the highest reduction in autogenous shrinkage as compared to all other mixes: a 32% decrease as compared to the reference mix XA-CA is observed at an age older than 100 days. The mix with alumina nanofibres, XA-CA_ANF, shows 16% reduction in shrinkage at the same age.

Similar trends to autogenous shrinkage are observed also for the total drying shrinkage for the effects on nanoparticles.

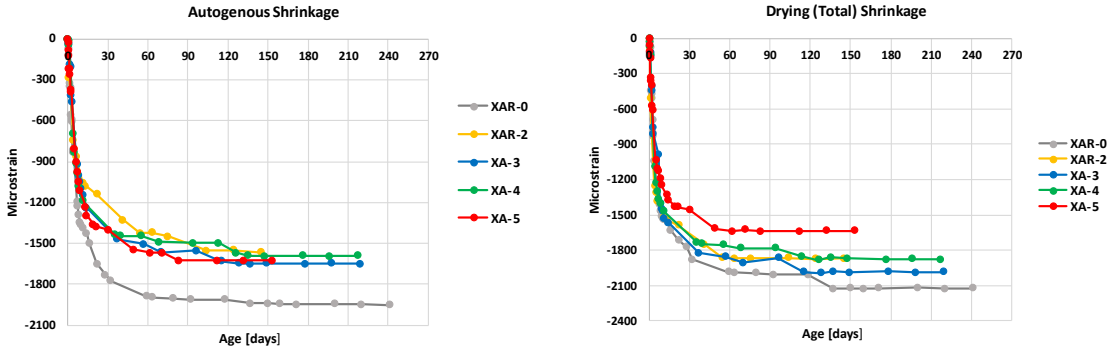

(a) *(b)*

Figure 3. (a) Autogenous shrinkage; (b) Drying (total) shrinkage.

3.3 Sorptivity tests and healing performance

The resistance of the investigated mixes against water transport was analyzed through capillary suction tests based on EN 13057. The method considers the increase in the mass of the concrete due to the capillary absorption of water over a fixed time interval.

As expected, the presence of the crack increases the water capillary suction of the concretes as can be shown in Figure 4, comparing the un-cracked and cracked curves. Moreover, water capillary suction decreased when the crack was partially healed as Figure 4 also shows. The positive effect of the crack self-healing is appreciated. After 1 month of healing a 19% improvement was measured for the reference mix XA-CA, while the effect increases up to 40% for the mix with alumina nanofibers XA-CA+ANF and to 41% for the mix with cellulose nanocrystals XA-CA+CNC. This highlights the role of nanoadditions in promoting, through their water uptake, retention and release capacity to promote a more effective self-sealing of the cracks through delayed hydration reactions.

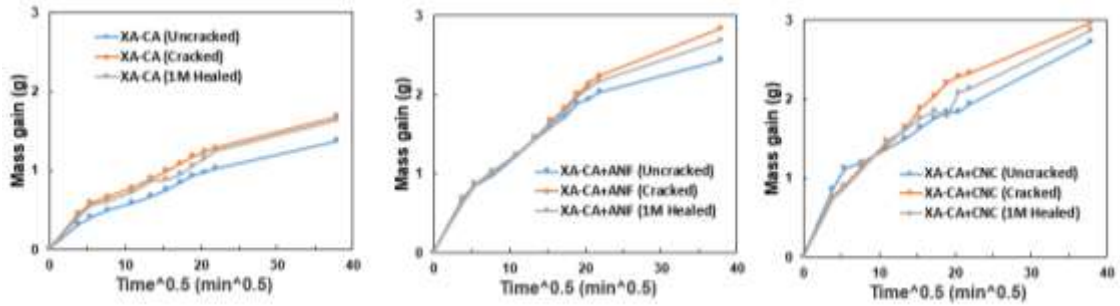

Figure 4. Mass gain (g) vs time$^{0.5}$ (min $^{0.5}$) curve for the uncracked, cracked and 1 month healed phase XA-CA, XA-CA+ANF, and XA-CA+CNC concretes immersed in geothermal water.

The self-healing performance of pre-cracked specimens were determined after one month. Two self-healing conditions were considered: 1) permanent immersion in geothermal water and 2) wet/dry cycles (immersion in geothermal water for 3 days, followed by air exposure for 2 days).

For the calculation of the Sealing Efficiency (SE), through water sorptivity test, the average (3 uncracked specimens, 3 cracked specimens and 3 healed specimens) of Sorption Coefficient (SC) values calculated as the slope of the experimental line of mass gain (g) versus time were used and the following equation was employed to determine the Sealing Efficiency (SE):

$$SE\ (\%) = \frac{SC_{cracked} - SC_{healed}}{SC_{cracked} - SC_{uncracked}} \cdot 100$$

The crack self-sealing capacity of the concretes was also quantified through microscopy observation as above. The self-sealing was assessed comparing how the crack area changes after certain healing period. To measure the crack area a digital microscope was used with a magnification factor of 45x for specimen bottom surfaces and 205x for side surfaces. To obtain a full representation of each crack 10-12 pictures from different spots were taken and then collated together using image-editing software (Figure 5-6). The procedure to obtain crack geometry parameters, either in terms of crack width or crack area is described in detail by *Cuenca et al*. (2018). Once such geometrical parameters have been calculated, the Crack Sealing Index is defined as:

$$Crack\ Sealing\ (\%) = \left(1 - \frac{w_t}{w_{initial}}\right) \cdot 100$$

where $w_{initial}$ is the initial crack width and w_t is the width of the same crack measured after a certain healing/conditioning time *t*.

The crack sealing (%) of the specimens subjected to wet/cycles and immersed in geothermal water for XA-CA, XA-CA+ANF, and XA-CA+CNC mixes are shown in Figure 7 (a) and Figure (b) respectively. For specimens subjected to wet/dry cycles a 40-50% sealing of the cracks was observed for specimens with nanoadditions whereas only 9% was observed for specimens without nanoadditions. Moreover, when specimens were immersed in geothermal water the sealing was 35-45% for concretes with nanoadditions and 20% for specimens without nanoadditions.

The average Sealing Efficiency (SE) calculated from the sorptivity tests and crack sealing (%) observed from visual crack analysis for specimens subjected to 1 month healing in geothermal water are correlated in Figure 8, where the average of 3 specimens is represented in each point. A consistency between the results obtained employing the two different procedures can be clearly appreciated (Ferrara et al. 2018) and the aforediscussed effects on nano-additions in promoting faster and more efficient healing reac-

tions is confirmed.

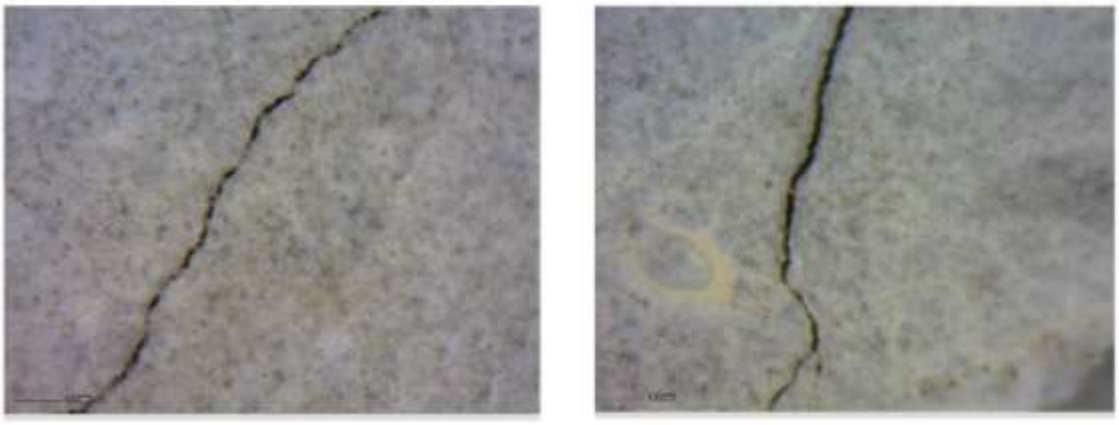

(a) *(b)*

Figure 5. Example of the induced cracks (images at x205 magnification).

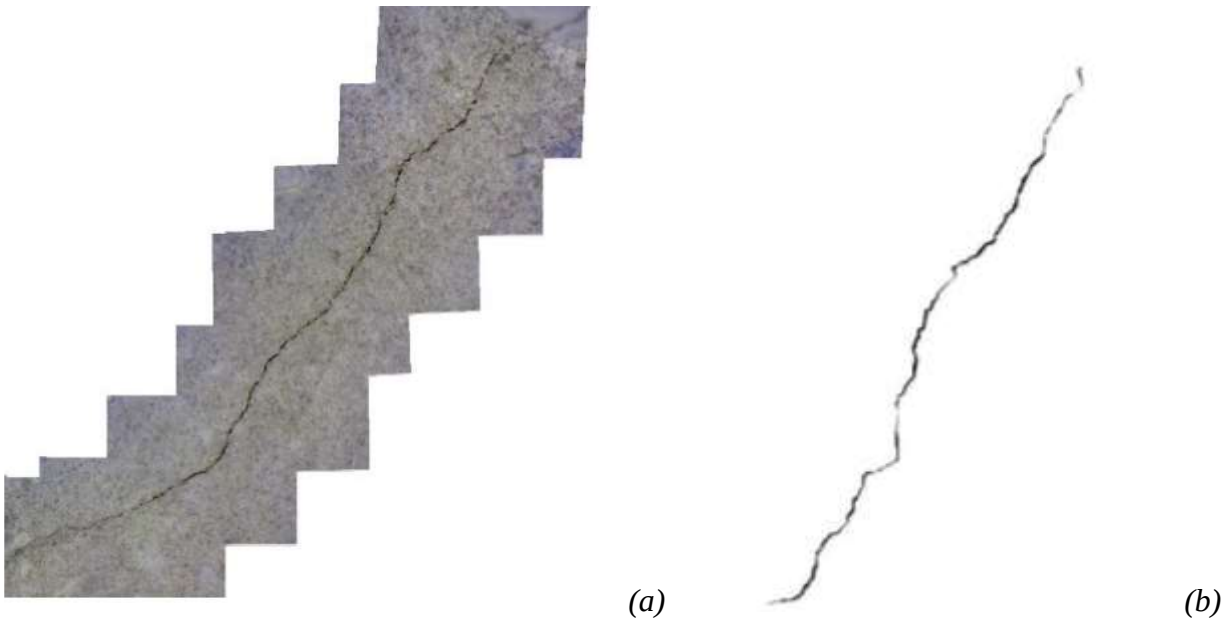

(a) *(b)*

Figure 6. (a) Example of the complete crack using an image-editing software and (b) black pixels representing the crack area.

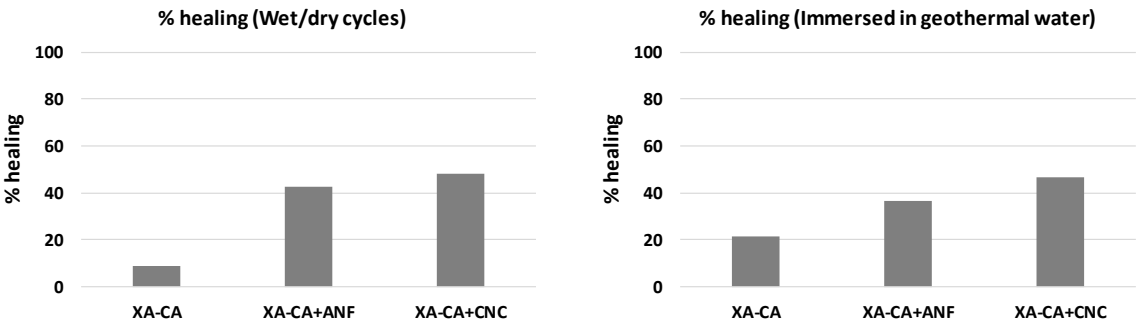

(a) *(b)*

Figure 7. % healing: (a) Specimens subjected to wet/dry cycles; (b) Specimens immersed in geothermal water.

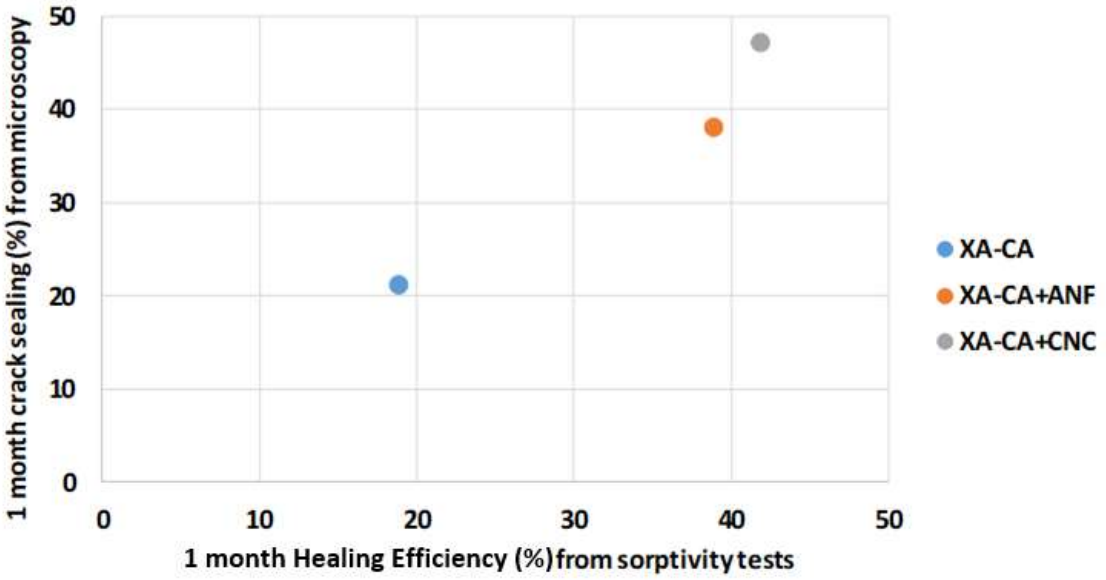

Figure 8. 1 month crack sealing (%) from microscopy vs 1 month Sealing Efficiency (%) from sorptivity tests.

4 CONCLUSIONS

In this paper the effects have been checked of alumina nano-fibers and cellulose nano-fibrils and nano-crystals on the mechanical and self-healing capacity of High Performance Fiber Reinforced Cementitious Composites when aging under conventional laboratory conditions and exposed to aggressive water containing chloride and sulfate ions. Such a condition has been meant as representative of infrastructures, such as water and mud basins, serving geothermal power plants and is specific of two of the pilots which will be built, with aforementioned cementitious composites, in the framework of H2020 Project ReSHEALience (GA 780624).

According to the results obtained from the present experimental campaign, nanoadditions are likely to improve the behavior of the UHDC in environments subjected to chemical attack (XA). It has been observed that nanoadditions confer to cementitious composites a better resistance against aging into sulfates rich environments (XA conditions) as compared to specimens cured in moist room. Specifically, the flexural strength of specimens immersed in geothermal water was higher for the mixes with nanoadditions. Regarding the shrinkage, nanoadditions also contributed to diminish the autogenous and drying shrinkage. This shrinkage reduction effect could be due to delayed hydration reactions, promoted, e.g., by some sort of internal curing capacity by the nanoparticles which further reduces the already minimal porosity of the matrices. Moreover, the capacity of nano-fibers to counteract the propagation of nano- and micro-scale defects from their very onset, can synergically with the aforementioned effect delay any kind of degradation phenomenon which the exposure to aggressive conditions may induce in the investigated composites.

The capillary suction coefficients were similar for all uncracked specimens (with and without nanoadditions), as due to extremely low porosity of all the investigated mixes.

The presence of alumina nanofibers and cellulose nanocrystals enhanced the self-sealing capability of the concrete. Self-sealing was analyzed determining the crack closure (%) by means of visual crack image processing. For specimens without nanoadditions the crack closure values were 9% and 20% for wet/dry cycles and immersion in geothermal water, respectively. With presence of nanoadditions, crack closure (%) im-

proved reaching higher crack closure percentages (between 35-50% for both curing conditions). This same effects was also confirmed by improved recovery of water-proofing, as witnessed by higher healing efficiency as quantified by means of sorptivity tests. The correlation between visually quantified crack sealing capacity and healing capacity measured via the recovery of the sorptivity coefficient contributes to support the reliability of the employed experimental procedures as well as the assessment of the nanoparticles effects.

ACKNOWLEDGEMENTS

The research activity reported in this paper has been performed in the framework of the ReSHEALience project (Rethinking coastal defence and Green-energy Service infrastructures through enHancEd-durAbiLity high-performance cement-based materials) which has received funding from the European Union's Horizon 2020 research and innovation program under grant agreement No 760824. The information and views set out in this publication do not necessarily reflect the official opinion of the European Commission.

The authors acknowledge the cooperation of MEng. Waqar Ahmed and MEng. Muhammad Awais in performing experimental tests, in partial fulfilment of the requirements for the MEng in Civil Engineering and Building Engineering respectively.

The kind collaboration of ReSHEALience partners ANF (dr. Alexej Tretjakov and dr. Dennis Lizunov), API-Europe (Mrs Stamatina Sideri and Dr. Evangelia Nteze) and Penetron Italia (Mr. EnricoMaria Gastaldo Brac) in supplyng respectively alumina nanofibres, cellulose nano-fibrils and crystals and the crystalline self-healing promoter is also acknowledged.

The authors also thank Mr. Marco Francini (BuzziUnicem) for supplying of cement, Mr. Michele Gadioli and Roberto Rosignoli (Azichem ltd) for supplying of steel fibres and Mr. Sandro Moro (BASF Italia) for supplying the superplasticizer employed for casting the different investigated UHDC mixes.

REFERENCES

Ahmed W. and Awais M. (2019), *Effects of nanoadditions on the performance of fiber reinforced cementitious composites in aggressive environments*, MS Dissertation defended on 16 April 2019 at the Politecnico of Milano, 146 p.

Borg, R.P., Cuenca, E., Gastaldo Brac, E.M. and Ferrara, L. (2018), *Crack sealing capacity in chloride rich environments of mortars containing different cement substitutes and crystalline admixtures*, Journal of Sustainable Cement Based Materials, V. 7(3), 141-159.

Buttignol T.E.T., Sousa J. L.A.O. and Bittencourt T.N. (2017), *Ultra High-Performance Fiber-Reinforced Concrete (UHPFRC): a review of material properties and design procedures*, IBRACON Structures and Materials Journal, V.10, No.4, 957-971.

Cuenca E., Criado M., Giménez M., Gastaldo Brac E.M., Sideri S., Tretjakov A., Alonso M.C. and Ferrara L. (2019), *Concept of Ultra High Durability Concrete for improved durability in chemical environments: Preliminary results*, Conference on Durable Concrete for Infrastructure under Severe Conditions - Smart admixtures, self-responsiveness and nano-additions, Ghent, Belgium.

Cuenca, E.A. and Ferrara, L. (2017), *Self-healing capability of Fiber Reinforced Concretes. State of the art and perspectives*, Journal of the Korean Society of Civil Engineers, V. 21(7), 2777-2789.

Cuenca E., Tejedor A. and Ferrara L. (2018), *A methodology to assess crack-sealing effectiveness of crystalline admixtures under repeated cracking-healing cycles*, Construction and Building Materials, V.179, 619-632.

Cuenca, E., Rigamonti, S., Gastaldo Brac, E. and Ferrara, L. (2019), *Improving resistance of cracked concrete to chloride diffusion through "healing stimulating" crystalline admixtures*, submitted for publication to Materials and Structures, March 29, 2019; revised version submitted June 27, 2019.

Ferrara, L., Krelani, V. and Carsana, M (2014), *A fracture testing based approach to assess crack healing of concrete with and without crystalline admixtures*, Construction and Building Materials, V. 68, 515-531.

Ferrara, L., Krelani, V. and Moretti, F. (2016), *On the use of crystalline admixtures in cement based construction materials: from porosity reducers to promoters of self-healing*, Smart Materials and Structures, V. 25 084002 (17pp).

Ferrara, L., Van Mullem, T., Alonso, M.C., Antonaci, P., Borg, R.P., Cuenca, E., Jefferson, A., Ng, P.L., Peled, A., Roig, M., Sanchez, M., Schroefl, C., Serna, P., Snoeck D., Tulliani, J.M. and De Belie, N. (2018), *Experimental characterization of the self-healing capacity of cement based materials and its effects on the material performance: a state of the art report by COST Action SARCOS WG2*, Construction and Building Materials, V. 167, 115-142.

Matthews S. (2007), *CON-REP-NET: Performance-based approach to the remediation of reinforced concrete structures: Achieving durable repaired concrete structures*. Journal of Building Appraisal, V.3, No.1, 6-20.

Serna P., Lo Monte F., Mezquida-Alcaraz E. J., Cuenca E., Mechtcherine V., Reichardt M., Peled A., Regev O., Borg R.P., Tretjakov A., Lizunov D., Sobolev K., Sideri S., Nelson K., Gastaldo Brac E.M. and Ferrara L. (2019), *Upgrading the concept of UHPFRC for high durability in the cracked state: the concept of Ultra High Durability Concrete (UHDC) in the approach of the H2020 project ReSHEALience*, RILEM SMSS, Rovinj, Croatia.